
Predicting Future Utility: Global Combinatorial Optimization for Task-Agnostic KV Cache Eviction

Ziyao Tang^{*123} Pengkun Jiao^{*1} Xinhang Chen² Wei Liu² Shiyong Li² Jingjing Chen¹

Abstract

Given the quadratic complexity of attention, KV cache eviction is vital to accelerate model inference. Current KV cache eviction methods typically rely on instantaneous heuristic metrics, implicitly assuming that score magnitudes are consistent proxies for importance across all heads. However, this overlooks the **heterogeneity in predictive fidelity** across attention heads. While certain heads prioritize the *instantaneous contribution* of tokens, others are dedicated to capturing *long-horizon utility*. In this paper, we propose that optimal budget allocation should be governed by the marginal utility in preserving long-term semantic information. Based on this insight, we propose LU-KV, a novel framework that optimizes head-level budget allocation through a convex-hull relaxation and a marginal-utility-based greedy solver to achieve near-optimal precision. Furthermore, we implement a data-driven offline profiling protocol to facilitate the practical deployment of LU-KV. Extensive evaluations on LongBench and RULER benchmarks demonstrate that **LU-KV** achieves an 80% reduction in KV cache size with minimal performance degradation, while simultaneously reducing inference latency and GPU memory footprint.

1. Introduction

The advent of Large Language Models (LLMs) has revolutionized long-context processing; however, the Key-Value (KV) cache presents a formidable bottleneck. As sequence lengths reach million-token scales, the linear growth of cache memory limits inference throughput and complicates scalable deployment. To address this, KV cache eviction (Zhang et al., 2023; Feng et al., 2024; Kim et al., 2025) has become a standard necessity, traditionally operating via

¹Fudan University ²Baidu ³Work done during an internship at Baidu. Correspondence to: Jingjing Chen <chenjingjing@fudan.edu.cn>.

a two-stage paradigm: *intra-head scoring* to identify critical tokens and *cross-head budget allocation* to distribute available storage across the model’s architecture.

While significant progress has been made in designing sophisticated scoring metrics (Zhang et al., 2023; Li et al., 2024), budget allocation strategies remain a critical yet underdeveloped frontier. Existing methods largely rely on **instantaneous heuristic scoring**, assuming that current attention magnitudes serve as reliable proxies for future importance. However, we identify a fundamental flaw in this magnitude-based paradigm: it ignores the inherent **heterogeneity in predictive fidelity** across different attention heads. Specifically, high-magnitude scores in certain heads often align poorly with **Oracle Importance**—the true long-term contribution to the KV cache—capturing transient noise rather than enduring semantic anchors. Blindly biasing budgets toward regions with high-magnitude heuristic scores, without accounting for their long-term utility, inevitably leads to suboptimal cache retention.

We posit that optimal budget allocation should be governed not by absolute scores, but by the **marginal utility** of a metric in preserving future information. In this view, memory allocation is treated as a strategic investment: if a metric exhibits poor alignment with the Oracle Importance in a specific head, increasing its budget yields rapidly diminishing returns. Conversely, in heads where the metric is precise, a unit investment in budget effectively preserves the model’s long-horizon generative quality. Therefore, the crux of an efficient allocation strategy lies in quantifying and optimizing the long-term cost-benefit ratio of each head under a specific metric.

Based on this insight, we propose **Long-horizon Utility KV (LU-KV)**, a novel framework for head-wise KV cache budget allocation. We introduce a data-driven offline calibration mechanism to profile the **marginal contribution curves** of individual attention heads. Based on this, we formulate the global budget distribution as a combinatorial optimization problem aimed at maximizing expected long-horizon utility retention across all heads. To solve this efficiently, we employ a **convex-hull relaxation** and a greedy solver, ensuring near-optimal budget allocation with minimal computational overhead.

Extensive experiments on the LongBench and RULER benchmarks demonstrate the effectiveness of **LU-KV**. Our method achieves an 80% reduction in KV cache size with minimal performance degradation, while simultaneously reducing inference latency and GPU memory footprint.

Our contributions are summarized as follows:

- We define the **Optimality Gap** between heuristic metrics and long-horizon utility importance, demonstrating that heuristic score magnitudes are insufficient for cross-head budget allocation.
- We formulate budget allocation as a global utility maximization problem and introduce an efficient solver using **convex-hull relaxation** and **marginal-utility-based greedy allocation**.
- We propose an **offline profiling protocol** that leverages the structural stability of LLMs, enabling **zero-overhead** online execution via a pre-computed lookup table.
- We conduct extensive evaluations across diverse long-context benchmarks to validate the effectiveness and robustness of our proposed methods.

2. Related Work

Existing research on KV cache eviction can be broadly categorized into two synergistic streams: *intra-head eviction policies*, which identify informative tokens within individual heads, and *cross-head budget allocation*, which manages resource distribution across the entire model.

Intra-head Eviction Policies Intra-head strategies focus on designing high-fidelity *proxy metrics* to distinguish critical tokens from noise. Early heuristics, such as StreamingLLM (Xiao et al., 2024), identified the “attention sink” phenomenon, showing that retaining initial tokens is crucial for maintaining model stability. Subsequently, methods like H2O (Zhang et al., 2023) and SnapKV (Li et al., 2024) utilized accumulated attention scores or observation windows to dynamically cluster and retain salient tokens. Beyond raw attention weights, recent literature has explored geometric and perturbation-based indicators to mitigate inherent biases. For instance, KeyDiff (Park et al., 2025) leverages the geometric features of Key vectors, while CriticalKV (Feng et al., 2025) explicitly measures potential output perturbations by considering Value magnitudes and projection weights. Despite their progress, these works primarily aim to optimize token selection within a fixed budget, often overlooking how that budget should be partitioned across heads.

Cross-Head Budget Allocation Recognizing the heterogeneity of information density across layers, recent studies have shifted toward non-uniform allocation strategies. **Static and rule-based methods** often rely on structural pri-

ors; for example, PyramidKV (Cai et al., 2024) employs a fixed pyramidal shape based on the “information funneling” hypothesis, while HeadKV (Fu et al., 2025) and CAKE (Qin et al., 2025) incorporate task-specific priors or spatial dispersion to formulate cascading rules. In contrast, **dynamic allocation strategies** like Ada-KV (Feng et al., 2024) attempt to distribute resources based on real-time statistics, such as attention entropy. However, these approaches inherently assume that proxy scores are well-calibrated and comparable across different heads—an assumption that often fails in practice due to varying score scales and metric inaccuracies.

Relation to our work. Unlike previous methods that rely on instantaneous heuristic scoring and consequently overlook the long-horizon importance of tokens, we propose an allocation framework governed by **Long-Horizon Utility**. Rather than directly comparing uncalibrated proxy scores, our approach profiles the offline budget-utility relationship to explicitly quantify the marginal gain of retaining tokens within each specific head. This grants our framework metric-universality: for any chosen proxy (e.g., SnapKV), we can derive the optimal budget configuration to maximize long-horizon information retention.

3. Preliminaries

We consider decoder-only LLMs with L layers and H attention heads per layer. Inference proceeds in two phases: parallel *prefill* and autoregressive *decoding*.

3.1. Attention Mechanism and KV Cache

At decoding step k , for a fixed layer ℓ and head h , the model generates a query $\mathbf{q}_{\ell,h,k} \in \mathbb{R}^{d_h}$ to attend to historical keys $\mathbf{k}_{\ell,h,j}$ and values $\mathbf{v}_{\ell,h,j}$ ($j \leq k$). The attention weights A and the head output are computed as:

$$A_{\ell,h,k,j} = \text{Softmax} \left(\frac{\mathbf{q}_{\ell,h,k}^\top \mathbf{k}_{\ell,h,j}}{\sqrt{d_h}} \right), \quad (1)$$

$$\mathbf{o}_{\ell,k} = \sum_{h=1}^H \left(\sum_{j=1}^T A_{\ell,h,k,j} \mathbf{v}_{\ell,h,j} \right) \mathbf{W}_O^{(\ell,h)}. \quad (2)$$

where $\mathbf{W}_O^{(\ell,h)} \in \mathbb{R}^{d_h \times d_{\text{model}}}$ is the head-specific output projection. To avoid redundant computation, previously computed (\mathbf{k}, \mathbf{v}) pairs are stored in a **KV Cache**. As the sequence length grows, the linear increase in cache size poses a significant memory bottleneck.

3.2. KV Cache Eviction

To maintain a manageable memory footprint, *KV Cache Eviction* strategies (Feng et al., 2024; Park et al., 2025)

impose a fixed budget B per head. These methods typically use attention scores as an importance proxy, retaining a subset of indices $\mathcal{I}_{\ell,h} \subset \{1, \dots, T\}$ such that $|\mathcal{I}_{\ell,h}| \leq B$. The attention output is then approximated by re-normalizing weights over the retained set:

$$\tilde{\mathbf{o}}_{\ell,h,k} = \sum_{j \in \mathcal{I}_{\ell,h}} \tilde{A}_{\ell,h,k,j} \mathbf{v}_{\ell,h,j}. \quad (3)$$

Current policies often prioritize ‘‘heavy hitters’’ with the highest cumulative attention scores, assuming their dominance in preserving model performance.

Symbol	Description
(ℓ, h)	The h -th attention head in the ℓ -th layer.
T	The total number of input tokens during the prefill phase.
π	The metric used to evaluate token importance.
π^*	The oracle metric of token importance.
σ	Target compression ratio (percentage of tokens evicted).
B_{total}	Global memory budget (total number of KV pairs to retain).
$b(\ell, h)$	Memory budget allocated to a specific attention head (ℓ, h) .
$\mathcal{M}_{\ell,h}^{\pi}$	Token indices at head (ℓ, h) , sorted by π (descending).
$\mathcal{M}_{\ell,h}^{\pi}(k)$	Pruned subset containing the top- k elements of $\mathcal{M}_{\ell,h}^{\pi}$.

4. Methodology

4.1. Long-horizon KV Cache Eviction

KV Cache eviction inherently entails a risk of information loss. Traditional eviction methods (e.g., H2O, SnapKV) rely on *instantaneous* attention weights, such as those calculated during the prefill stage. We term these methods **Heuristic Metric**. However, these methods overlook the potential for shifts in attention patterns during future decoding steps. To address this, we propose **Long-horizon Utility KV (LU-KV)**, a framework that evaluates KV utility over extended sequences. We formulate the cache eviction problem as a Global Combinatorial Optimization of long-horizon utility, which we solve to determine the optimal head-wise budget allocation.

Oracle Importance. To strictly quantify the importance of a token, we need a definitive standard of token utility based on actual contribution for model inference. Inspired by the output perturbation bound analysis in AdaKV (Feng et al., 2024) and the criticality definition in CriticalKV (Feng et al., 2025), we posit that true token importance should reflect its actual contribution to the final model output.

Accordingly, we define the **Oracle Importance** $I_{\ell,h,j}$ of a cached position j in head (ℓ, h) as its maximum potential contribution over a future decoding window:

$$I_{\ell,h,j} \triangleq \max_{k \in \{1, \dots, K_{\text{max}}\}} \left(A_{\ell,h,k,j} \cdot \left\| \mathbf{v}_{\ell,h,j} \mathbf{W}_O^{(\ell,h)} \right\| \right). \quad (4)$$

This metric captures the true utility of a token in a long-horizon view: whether it constitutes a major component of

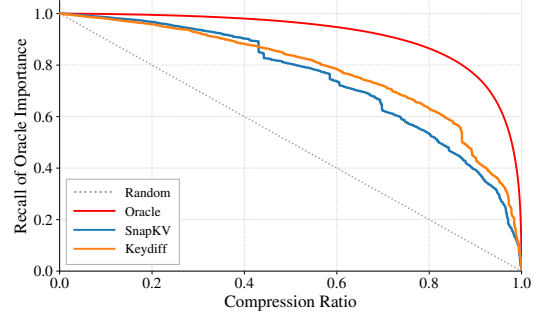


Figure 1. Recall of oracle importance for oracle metric and several heuristic metrics across varying compression ratios (σ), where 1 implies full compression and 0 implies no compression.

the output vector at any future step k . Based on this, we theoretically construct an **Oracle Metric** (π^*) that yields the set $\mathcal{M}_{\ell,h}^{\pi^*}$, which perfectly aligns with the descending ranking of the ground-truth oracle importance $I_{\ell,h,\cdot}$.

Limitation of Heuristic Metric. Considering a head KV cache budget $b_{\ell,h}$. In practice, however, $\mathcal{M}_{\ell,h}^{\pi}(b_{\ell,h})$ determined by a heuristic metric π often deviates from the optimal set $\mathcal{M}_{\ell,h}^{\pi^*}(b_{\ell,h})$, due to the short-horizon of π .

To analyze this discrepancy, we decompose the relationship between $\mathcal{M}_{\ell,h}^{\pi^*}$ and $\mathcal{M}_{\ell,h}^{\pi}$ into 3 classes:

- **Hits:** $\mathcal{M}_{\ell,h,\text{hit}} = \mathcal{M}_{\ell,h}^{\pi^*}(b_{\ell,h}) \cap \mathcal{M}_{\ell,h}^{\pi}(b_{\ell,h})$ (Correctly retained high oracle importance tokens)
- **Misses:** $\mathcal{M}_{\ell,h,\text{miss}} = \mathcal{M}_{\ell,h}^{\pi^*}(b_{\ell,h}) \setminus \mathcal{M}_{\ell,h}^{\pi}(b_{\ell,h})$ (High Oracle importance, wrongly evicted)
- **False Positives:** $\mathcal{M}_{\ell,h,\text{fp}} = \mathcal{M}_{\ell,h}^{\pi}(b_{\ell,h}) \setminus \mathcal{M}_{\ell,h}^{\pi^*}(b_{\ell,h})$ (Low oracle importance, wrongly retained)

Consequently, kept cache set $\mathcal{M}_{\ell,h}^{\pi}(b_{\ell,h})$ determined by π can also be expressed as:

$$\mathcal{M}_{\ell,h}^{\pi}(b_{\ell,h}) = (\mathcal{M}_{\ell,h}^{\pi^*}(b_{\ell,h}) \setminus \mathcal{M}_{\ell,h,\text{miss}}) \cup \mathcal{M}_{\ell,h,\text{fp}}. \quad (5)$$

Let **eviction loss** $\mathcal{L}_{\ell,h}(\cdot)$ denote the Oracle Importance mass lost by head (ℓ, h) due to the removal of kv cache.

$$\mathcal{L}_{\ell,h}(\mathcal{M}_{\ell,h}) \triangleq \sum_{j \notin \mathcal{M}_{\ell,h}} I_{\ell,h,j}. \quad (6)$$

Substituting the set formulation from Eq. (5) into the loss definition in Eq. (6), we can rigorously decompose the eviction loss of policy π into two distinct components:

$$\begin{aligned} \mathcal{L}_{\ell,h}(\mathcal{M}_{\ell,h}^{\pi}(b_{\ell,h})) &= \mathcal{L}_{\ell,h}(\mathcal{M}_{\ell,h}^{\pi^*}(b_{\ell,h})) + \sum_{j \in \mathcal{M}_{\ell,h,\text{miss}}} I_{\ell,h,j} - \sum_{j \in \mathcal{M}_{\ell,h,\text{fp}}} I_{\ell,h,j} \\ &= \underbrace{\mathcal{L}_{\ell,h}(\mathcal{M}_{\ell,h}^{\pi^*}(b_{\ell,h}))}_{\text{Loss of Oracle Metric}} + \underbrace{\Delta_{\ell,h}(\pi, \pi^*, b(\ell, h))}_{\text{Optimality Gap}}. \end{aligned} \quad (7)$$

where $\mathcal{L}_{\ell,h}(\mathcal{M}_{\ell,h}^*)$ is the eviction loss of Oracle Metric, which is fixed due to compression ratio; $\Delta_{\ell,h}(\pi, I)$ is defined as the **Optimality Gap** between the oracle metric and the used metric π in long-horizon view, which relevant to π .

Figure 1 validates the decomposition in Eq. (7) by visualizing the total loss as the vertical distance to $Recall = 1.0$. Specifically, the loss of a heuristic metric $\mathcal{L}_{\ell,h}(\mathcal{M}_{\ell,h}^\pi(b_{\ell,h}))$ is the sum of the inherent **Oracle loss** (red curve to 1.0) and the **Optimality Gap** (vertical gap between heuristic metric curve and oracle curve). This observation suggests two optimization paths: (1) refining budget allocation cross head to lower the total Oracle loss, and (2) improving the selection metric to bridge the optimality gap.

4.2. Global Optimization of Head-Level KV Cache Budget Allocation

The formulation above characterizes the loss within a single attention head; however, modern LLMs operate through a complex **multi-head, multi-layer** architecture. Existing *head-level* approaches, e.g. AdaKV (Feng et al., 2024), attempt to address this by employing a global greedy strategy that pools candidate tokens from all heads and retains the top- K elements based on surrogate scores. Nevertheless, this strategy remains suboptimal due to the existence of the **Optimality Gap** $\Delta_{\ell,h}(\pi, \pi^*, b(\ell, h))$ defined in Eq. 7.

Global Optimization Objective. We now consider the problem of allocating a global cache budget B_{total} across all attention heads to minimize the aggregate eviction loss across the entire model.

Let $b_{\ell,h}$ denote the cache budget allocated to head (ℓ, h) , subject to the global constraint $\sum_{\ell,h} b_{\ell,h} = B_{\text{total}}$. For a given metric π , we define $\mathcal{M}_{\ell,h}^\pi(b_{\ell,h})$ as the set of top- $b_{\ell,h}$ token positions selected by π within that head.

The global optimization objective aims to minimize the aggregate eviction loss across all layers and heads by optimizing the budget distribution $\{b_{\ell,h}\}$:

$$\begin{aligned} \min_{\{b_{\ell,h}\}} \quad & \sum_{\ell=1}^L \sum_{h=1}^H \mathcal{L}_{\ell,h}(\mathcal{M}_{\ell,h}^\pi(b_{\ell,h})), \\ \text{s.t.} \quad & \sum_{\ell=1}^L \sum_{h=1}^H b_{\ell,h} = B_{\text{total}}. \end{aligned} \quad (8)$$

Since $\mathcal{M}_{\ell,h}^\pi(b_{\ell,h})$ lacks strict monotonicity with respect to the oracle importance, and given that the parameter space for $\{b_{\ell,h}\}$ constitutes a high-dimensional combinatorial domain, rendering the global optimization problem NP-hard. The proof of the non-convex of $\mathcal{L}_{\ell,h}(\mathcal{M}_{\ell,h}^\pi(b_{\ell,h}))$ is provided in Appendix A.1.

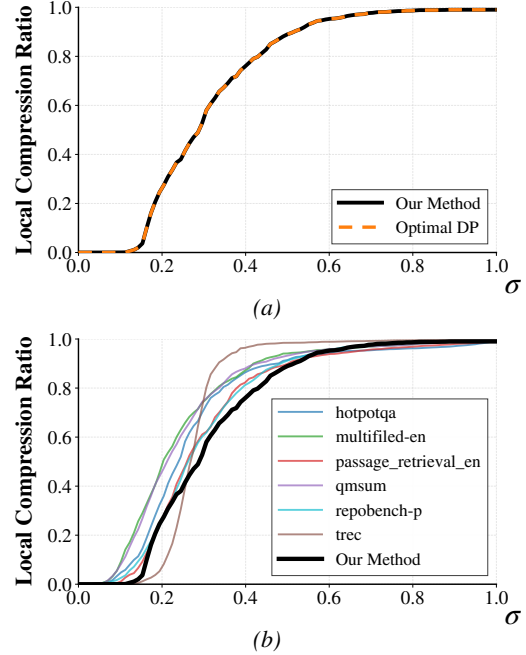


Figure 2. (a) Comparison between our greedy solver based on convex-hull relaxation (solving Eq. 10) and DP solution (solving Eq. 8). (b) Shows the consistent trend of optimal local compression ratio across different downstream tasks under the same global compression ratio σ .

Efficient Optimization via Convex Hull Relaxation.

To facilitate an efficient solution to the objective in Equation 8, we propose a convex relaxation approach that transforms the discrete loss $\mathcal{L}_{\ell,h}$ into a tractable surrogate. By applying Isotonic Regression via the Pool Adjacent Violators Algorithm (PAVA) to the raw loss sequence $\{\mathcal{L}_{\ell,h}(\mathcal{M}_{\ell,h}^\pi(i)) \mid 1 \leq i \leq T\}$, we derive a convex, non-increasing surrogate sequence, denoted as $\{\check{\mathcal{L}}_{\ell,h}(\mathcal{M}_{\ell,h}^\pi(i)) \mid 1 \leq i \leq T\}$. We define the **Effective Marginal Gain** of allocating i -th token in $\mathcal{M}_{\ell,h}^\pi$:

$$g_{\ell,h}^\pi(i) = \check{\mathcal{L}}_{\ell,h}(\mathcal{M}_{\ell,h}^\pi(i-1)) - \check{\mathcal{L}}_{\ell,h}(\mathcal{M}_{\ell,h}^\pi(i)) \geq 0. \quad (9)$$

The marginal gain $g_{\ell,h}^\pi(i)$ is monotonically non-increasing while i increases. This property allows a global greedy strategy to achieve the global optimum for the *relaxed* objective:

$$\begin{aligned} \min_{\{b_{\ell,h}\}} \quad & \sum_{\ell=1}^L \sum_{h=1}^H \check{\mathcal{L}}_{\ell,h}(\mathcal{M}_{\ell,h}^\pi(b_{\ell,h})), \\ \text{s.t.} \quad & \sum_{\ell=1}^L \sum_{h=1}^H b_{\ell,h} = B_{\text{total}}. \end{aligned} \quad (10)$$

Specifically, we iteratively allocate the i -th token from the attention head (ℓ, h) that yields the maximum effective marginal gain $g_{\ell,h}^\pi(i)$, continuing until the global budget B_{total} is exhausted. As illustrated in Figure 2a, our approach

achieves an exact match with the results of the optimal Dynamic Programming (DP) solver. Details of the convex relaxation and allocation process are in Appendix A.2.

4.3. Practical Implementation: Offline Profiling

The optimization problem formulated in Eq. 10 requires future decoding results to compute the oracle importance I , which is inherently inaccessible during real-time inference.

However, we identify a key structural property of LLMs: individual attention heads exhibit a **consistent trend** in their optimal local-to-global compression ratios across diverse tasks. As illustrated in Figure 2b, these compression profiles remain remarkably stable across various scenarios, e.g. question answering and long-context retrieval. This empirical consistency allows us to characterize the optimal global-local budget allocation in an offline manner.

Offline Optimal Budget Estimation. To construct this offline allocation, we employ a data-driven probing protocol consisting of three phases:

- **Context Generation:** We construct a long-context input $C_{\text{syn}} (\approx 4,000$ tokens) with a coherent narrative structure to simulate realistic KV cache states.
- **Oracle Computation:** We generate a diverse set of queries $\mathcal{Q} = \{q_1, \dots, q_M\}$ targeting different information segments. For each q_i , the ground-truth oracle importance is computed via full-attention decoding.
- **Profile Aggregation:** We solve Eq. 10 for each query across a dense grid of global compression ratios $\rho \in [0, 1]$ to obtain the query-specific optimal local ratios $r_{\ell,h}^{*(\pi)}(q_i; \rho)$.

We aggregate these solutions into a final static profile $\Phi^{(\pi)}$ by averaging the optimal local ratios across the calibration set:

$$\Phi^{(\pi)}(\rho)_{\ell,h} \triangleq \frac{1}{M} \sum_{i=1}^M r_{\ell,h}^{*(\pi)}(q_i; \rho). \quad (11)$$

The resulting $\Phi^{(\pi)}$ serves as a lookup table mapping any target global sparsity ρ to a precise configuration for every head, effectively capturing the **expected utility** of each head across the general data distribution.

Online Execution. During inference, our method introduces negligible computational overhead through three steps:

1. **Lookup:** Given a target global compression ratio σ_{target} , the system retrieves the pre-computed local ratios $\{r_{\ell,h}\} \leftarrow \Phi^{(\pi)}(\sigma_{\text{target}})$.
2. **Budgeting:** These ratios are translated into integer budgets: $b_{\ell,h} = \lfloor (1 - r_{\ell,h}) \cdot T \rfloor$.

3. **Eviction:** Each head independently applies the heuristic metric π to retain the top- $b_{\ell,h}$ tokens.

This strategy successfully bridges the gap between theoretical oracle performance and practical runtime constraints without requiring online optimization.

5. Experiments

5.1. Experimental Setup

Benchmarks. We assess general long-context generation capabilities using **LongBench** (Bai et al., 2024), which consists of 16 diverse datasets covering various long-form tasks. Additionally, we utilize **RULER** (Hsieh et al., 2024) to evaluate retrieval robustness across expanding context windows, ranging from 4k to 128k tokens. Further details regarding the benchmarks are provided in Appendix C.

Base Models and Baseline Methods. We evaluate our method using LLMs of varying scales and context window capacities: Llama-3.1-8B-Instruct (Dubey et al., 2024), Mistral-7B-Instruct-v0.3 (Jiang et al., 2023), and Qwen2.5-32B-Instruct (Team, 2024).

We consider two KV cache importance metrics: the **Metric SnapKV** (Li et al., 2024), denoted as π_1 , which relies on accumulated attention scores; and the **Metric KeyDiff** (Park et al., 2025), denoted as π_2 , which utilizes the geometric features of key vectors. Under these two metrics, we compare our approach against three allocation strategies:

- **Uniform:** A static allocation that distributes the KV budget evenly across all layers.
- **PyramidKV** (Cai et al., 2024): A static allocation based on the *Information Funneling* hypothesis, which progressively prunes the budget in deeper layers.
- **AdaKV** (Feng et al., 2024): A dynamic allocation employing **Global Top- k** selection, based on the assumption that heads with higher importance scores warrant larger budgets.

Detailed baseline specifications are deferred to Appendix D.

Experimental Settings. Our evaluations are conducted using the KVPress framework (NVIDIA, 2024), adopting a *question-agnostic* compression protocol. In this setting, the context is compressed and the KV cache is evicted solely based on the input document, strictly before the arrival of any query. This paradigm closely mirrors real-world production environments where the prompt or context is pre-filled and cached for future unknown user interactions. Furthermore, by precluding access to query-specific attention, this setup imposes a significantly more rigorous test on the method’s ability to retain salient information compared to query-aware approaches.

Predicting Future Utility: Global Combinatorial Optimization for Task-Agnostic KV Cache Eviction

Table 1. **Main Results on LongBench.** Comparison of KV cache eviction strategies using the SnapKV Metric (π_1) and the KeyDiff Metric (π_2) at an 80% compression ratio.

Model	Method	QA		Summ.	Few-Shot	Synth.	Code	Avg.
		Single	Multi					
Mistral B-v0.3	Full-KV	38.36	37.83	28.86	70.86	51.25	63.26	47.30
	Uniform- π_1	24.70	31.78	24.15	63.95	47.50	60.98	40.67
	Pyramid- π_1	25.36	31.95	23.98	63.35	48.75	61.80	40.94
	Ada- π_1	26.21	31.88	24.42	66.52	49.50	62.05	41.89
	LU-KV-π_1 (Ours)	37.16	36.59	27.97	69.81	51.35	57.69	45.79
	Uniform- π_2	28.53	30.86	24.71	59.00	33.08	46.89	36.83
	Pyramid- π_2	29.44	30.53	24.50	59.33	34.06	42.95	36.59
	LU-KV-π_2 (Ours)	39.80	38.09	28.22	68.32	52.02	56.04	46.21
Qwen 72B	Full-KV	42.91	54.15	27.33	68.91	55.75	42.35	48.51
	Uniform- π_1	25.02	44.50	23.33	64.45	48.75	44.99	41.21
	Pyramid- π_1	19.44	40.23	21.84	60.24	50.46	46.34	38.68
	Ada- π_1	25.75	43.60	23.34	65.70	50.13	44.97	41.58
	LU-KV-π_1 (Ours)	39.84	53.55	26.19	67.32	54.75	48.46	47.95
	Uniform- π_2	26.85	44.30	22.32	65.82	38.36	29.32	38.33
	Pyramid- π_2	22.00	35.87	20.64	60.05	24.71	26.85	32.42
	LU-KV-π_2 (Ours)	41.58	54.23	26.61	67.86	53.75	46.91	48.26

Table 2. **Main Results on RULER-16K.** Comparison of KV cache eviction strategies using the SnapKV Metric (π_1) and the KeyDiff Metric (π_2) at an 80% compression ratio.

Model	Method	RULER Tasks (16K)													
		single1	single2	single3	multkey1	multkey2	multkey3	multivalue	multiquery	vt	cwe	fwe	qa-1	qa-2	Avg
Mistral B-v0.3	Full-KV	94.20	96.40	99.60	97.40	95.60	76.80	89.50	88.65	96.28	82.22	87.93	71.60	50.00	86.63
	Uniform- π_1	40.40	16.20	2.40	14.20	6.20	1.00	9.65	11.00	66.92	66.96	85.53	29.80	33.60	29.53
	Pyramid- π_1	50.00	57.00	2.40	28.00	4.80	0.20	16.15	21.55	62.32	31.94	82.20	32.00	33.00	32.43
	Ada- π_1	58.00	38.80	2.40	20.20	12.40	5.60	12.85	16.80	92.08	71.36	86.13	33.60	37.00	37.48
	LU-KV-π_1 (Ours)	70.80	78.80	18.20	83.60	79.20	67.40	67.80	76.25	95.88	78.32	84.47	62.00	47.00	69.98
	Uniform- π_2	94.60	72.80	100.00	78.80	7.40	0.80	94.80	86.10	94.16	65.56	90.87	32.40	35.80	65.70
	Pyramid- π_2	93.20	96.20	99.60	88.20	6.60	0.60	92.00	89.75	94.36	36.92	88.73	31.40	34.80	65.57
	LU-KV-π_2 (Ours)	85.60	76.60	100.00	87.00	90.80	35.20	96.45	92.85	92.16	80.78	86.80	64.60	46.80	79.66
Qwen 72B	Full-KV	100.00	100.00	100.00	100.00	99.80	100.00	99.85	99.95	100.00	97.70	96.20	79.40	62.40	95.02
	Uniform- π_1	97.40	55.60	3.80	25.80	4.80	2.00	14.40	19.60	99.28	87.14	94.00	28.00	39.00	43.91
	Pyramid- π_1	83.80	36.00	2.40	19.20	2.00	0.00	13.15	14.95	93.68	56.84	95.73	26.40	34.60	36.83
	Ada- π_1	98.80	52.60	4.40	21.80	7.00	4.20	14.75	18.25	99.32	88.48	94.53	29.40	39.00	44.04
	LU-KV-π_1 (Ours)	99.80	99.20	32.00	84.20	71.80	78.40	84.60	85.80	99.72	95.66	93.13	65.00	56.80	80.47
	Uniform- π_2	100.00	100.00	100.00	100.00	8.00	1.00	99.40	99.95	98.92	90.36	99.33	36.40	41.40	74.98
	Pyramid- π_2	100.00	100.00	99.80	99.60	1.00	0.20	99.55	99.95	84.52	69.26	98.93	30.20	35.80	70.68
	LU-KV-π_2 (Ours)	100.00	100.00	100.00	100.00	44.20	23.00	99.00	99.90	99.88	95.34	99.07	44.00	46.40	80.81

5.2. Main Results on KV Cache Eviction

Results on LongBench. Table 1 summarizes the performance under an 80% compression ratio. Consistent with our global optimization objective in Eq. 8, our method effectively minimizes the aggregate eviction loss, translating into significant accuracy gains. On Mistral-7B-v0.3

with π_2 (KeyDiff), our method improves the average accuracy from 40.54 (AdaKV) to 46.21, recovering **84%** of the performance gap between the compressed model and the Full-KV upper bound. Crucially, these gains are robust across diverse domains—from summarization to synthetic tasks—demonstrating that our learned compression profiles

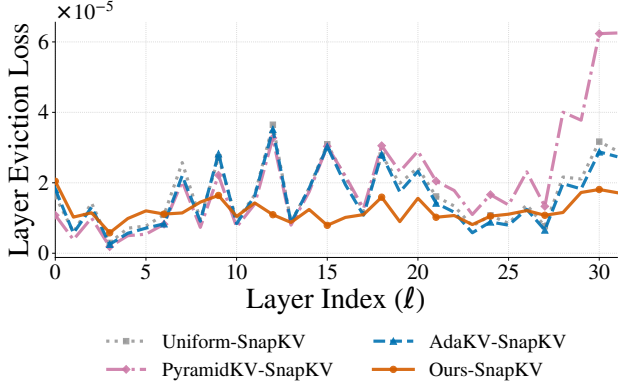


Figure 3. Comparison of aggregated layer-wise eviction loss. **Ours** consistently achieves the lowest and most stable loss across all layers, whereas baselines like AdaKV and PyramidKV exhibit severe loss spikes.

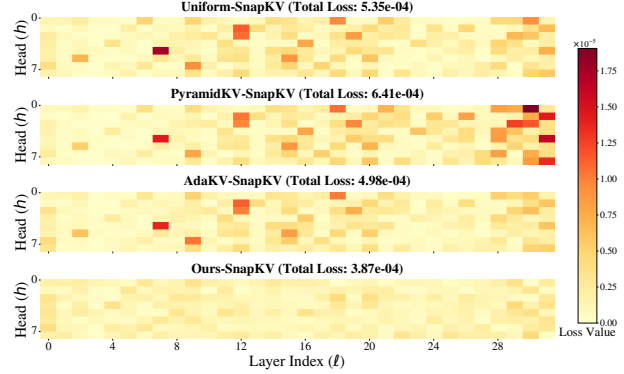
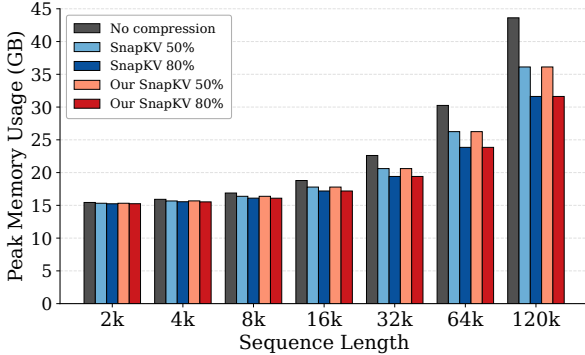
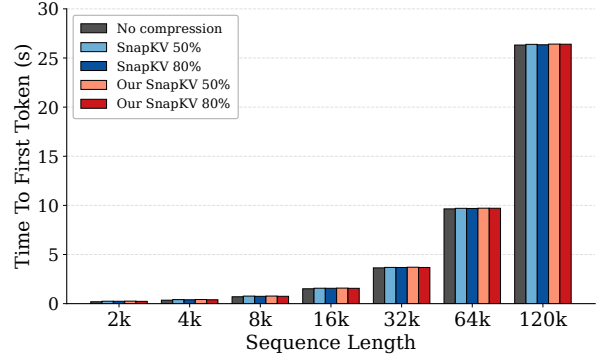


Figure 4. Heatmap visualization of per-head loss distribution $\mathcal{L}_{\ell,h}$. Baselines suffer from intense “loss bursts” (dark red blocks) in specific heads due to optimality gap, while our method effectively suppresses these spikes across the entire model.



(a) Peak memory usage



(b) Time To First Token (TTFT) latency

Figure 5. Efficiency comparison on Llama-3.1-8b. Our method maintains comparable latency to baselines while significantly reducing memory usage in long-context scenarios.

successfully capture the intrinsic *Oracle Importance* distribution across varying data densities.

Results on RULER. The RULER benchmark serves as a stress test for retrieval robustness in extreme contexts. Focusing on *Mistral-7B-v0.3* using the SnapKV metric (π_1) in Table 2, conventional strategies struggle significantly: Uniform allocation collapses to 29.53% average accuracy, and AdaKV provides only marginal relief at 37.48%. In contrast, our approach achieves a remarkable **69.98%** average accuracy under the same 80% compression ratio. Notably, on the challenging *multkey-3* task, our method boosts performance from 1.00% (Uniform) to 67.40%, demonstrating substantial robustness in preserving sparse yet critical information.

5.3. LU-KV is Optimal Global Allocation.

To validate our core hypothesis, we visualize the eviction loss distribution under an 80% compression ratio. As il-

lustrated in Figure 3 and Figure 4, the failure modes of different strategies reveal their fundamental limitations in both optimization granularity and deployment constraints.

Limitations of PyramidKV. PyramidKV primarily attempts to optimize in the layer-wise dimension based on fixed priors. While it adjusts the budget distribution across layers, Figure 3 (pink line) shows that this rigid heuristic induces a sharp escalation in loss within deeper layers (layers 27–32), failing to adapt to the high semantic density of these regions. Consequently, the aggressive pruning in deep layers—based on an ill-suited pyramidal hypothesis—causes irreversible context loss that outweighs the minor gains in shallow layers, ultimately yielding a higher aggregated Oracle Loss than the Uniform baseline.

Limitations of AdaKV. AdaKV focuses on the head-wise dimension, allocating budgets dynamically based on proxy score magnitudes. However, it faces a critical engineering trade-off: performing a true global cross-layer sort requires buffering all KV states during prefill, which causes unac-

Table 3. **Ablation Study on LongBench.** We evaluate the impact of the optimality gap by comparing strategies **w/o Optimality Gap** (Δ) against **w/ Optimality Gap**. Evaluated on **Mistral-7B-v0.3** and **Qwen2.5-32B** at an 80% compression ratio.

Model	Method	Single-Doc QA			Multi-Doc QA			Summarization			Few-shot			Synthetic		Code		Avg
		NrivQA	Qasper	MF-en	Hotpot	2WikiQA	Musique	CovRep	QMSum	MultiNews	TREC	TriviaQA	SAMSum	PCount	PR-en	Lcc	RB-P	
Mistral-7B	Full-KV	27.04	38.30	49.75	49.11	36.68	27.69	34.64	25.55	26.40	76.50	88.96	47.11	5.50	97.00	65.60	60.92	47.30
	LU-KV- π_1 (w/o Δ)	23.03	27.14	42.68	49.69	31.27	21.20	30.34	23.15	23.64	66.00	89.36	47.13	5.00	96.50	66.72	60.33	43.95
	LU-KV- π_1 (w/ Δ)	25.25	34.91	51.32	48.87	38.10	22.80	33.57	25.02	25.31	71.00	91.32	47.12	5.19	97.50	53.76	61.62	45.79
	LU-KV- π_2 (w/o Δ)	24.82	29.97	47.07	44.72	34.68	23.10	30.62	24.15	24.53	47.50	89.06	46.80	4.68	92.50	46.63	60.89	41.98
	LU-KV- π_2 (w/ Δ)	25.80	39.78	53.82	48.26	41.33	24.69	33.49	25.52	25.65	69.00	88.81	47.14	6.53	97.50	51.18	60.89	46.21
Qwen2.5-32B	Full-KV	30.68	45.93	52.13	63.00	60.75	38.71	32.43	24.51	25.06	72.00	88.71	46.01	11.50	100.00	50.72	33.98	48.51
	LU-KV- π_1 (w/o Δ)	27.50	26.07	36.90	59.58	53.91	37.27	29.37	20.76	22.32	65.50	88.57	45.45	9.50	99.25	60.36	37.77	45.00
	LU-KV- π_1 (w/ Δ)	29.41	39.16	50.95	62.82	58.00	39.84	31.34	23.12	24.10	71.00	88.89	42.07	9.50	100.00	60.21	36.71	47.95
	LU-KV- π_2 (w/o Δ)	26.65	26.11	42.18	57.12	52.08	30.64	28.25	22.33	21.16	73.50	88.69	43.64	8.50	91.54	42.14	36.31	43.18
	LU-KV- π_2 (w/ Δ)	31.30	42.88	50.55	61.61	59.67	41.41	31.56	24.01	24.25	74.00	88.31	41.28	7.50	100.00	55.45	38.37	48.26

ceptable peak memory spikes. Consequently, AdaKV is often practically constrained to layer-wise uniform (or locally dynamic) budgets while competing only within layers. This explains why its layer-wise loss curve (Figure 3, blue dashed line) closely mirrors the Uniform baseline, failing to rebalance resources across layers. Furthermore, within layers, Figure 4 reveals that distinct “loss bursts” (dark red blocks) persist. This confirms the ranking discordance: simply prioritizing heads with high proxy scores fails to capture true Oracle importance, leading to suboptimal intra-layer allocation.

Superiority of Allocation with Optimality Gap. Our method integrates the advantages of both dimensions while circumventing their drawbacks. As an offline static strategy, our method retrieves the optimal configuration from a pre-computed profile. This allows us to execute true global optimization (Cross-Layer & Cross-Head) without incurring the runtime memory overhead that limits online dynamic methods. Results show distinct improvements in two aspects: (1) Cross-Layer: Figure 3 (orange solid line) shows that our method effectively homogenizes the eviction loss across all layers, preventing the surge in deeper layers observed in PyramidKV. (2) Cross-Head: Figure 4 confirms that the localized “loss bursts” characteristic of AdaKV are successfully eliminated. By optimizing the Effective Marginal Gain ($g_{\ell,h}^{\pi}$) globally, we achieve superior resource utilization, significantly reducing the total Oracle Eviction Loss compared to AdaKV (3.87×10^{-4} vs. 4.98×10^{-4}).

5.4. Ablation Study

To deconstruct our performance gains, we evaluate two allocation logics in Table 3. The first, **Without Optimality Gap Allocation**, distributes the budget solely on total Oracle importance, assuming perfect metric ranking while ignoring

the Optimality Gap. The second, our **With Optimality Gap Allocation**, incorporates the correction term to rectify metric-oracle discrepancies.

Results show that disregarding the optimality gap causes a substantial performance degradation, with an average score decrease of **3.53** points. This validates our derivation: optimal allocation should not be dictated by where the proxy metric *perceives* importance (Method Confidence), but where it *accurately* preserves critical information (Method Correctness).

5.5. Efficiency

Figure 5 shows that on *Llama-3.1-8B*, our method achieves peak memory reduction and TTFT latency comparable to the SnapKV baseline. This confirms that our proposed method introduces negligible computational overhead, effectively maintaining strict resource limits while significantly mitigating the performance degradation caused by compression.

6. Conclusion

In this paper, we theoretically analyze the limitations of existing heuristic KV eviction methods through the lens of long-horizon inference, revealing their inability to capture the long-term cumulative contribution of tokens.

To bridge this gap, we introduce a novel paradigm: KV cache retention should be determined not only by instantaneous importance but also by future utility. We formulate the head-level budget allocation as a global combinatorial optimization problem and propose an efficient convex-hull relaxation and a greedy solver algorithm to solve it. Extensive evaluation across highly demanding benchmarks, such as LongBench and RULER, demonstrates the efficacy of our proposed approach.

References

- Bai, Y., Lv, X., Zhang, J., Lyu, H., Tang, J., Huang, Z., Du, Z., Liu, X., Zeng, A., Hou, L., et al. Longbench: A bilingual, multitask benchmark for long context understanding. In *Proceedings of the 62nd annual meeting of the association for computational linguistics (volume 1: Long papers)*, pp. 3119–3137, 2024.
- Cai, Z., Zhang, Y., Gao, B., Liu, Y., Liu, T., Lu, K., Xiong, W., Dong, Y., Chang, B., Hu, J., and Xiao, W. Pyramidkv: Dynamic KV cache compression based on pyramidal information funneling. *CoRR*, abs/2406.02069, 2024. doi: 10.48550/ARXIV.2406.02069. URL <https://doi.org/10.48550/arXiv.2406.02069>.
- Chen, M. Evaluating large language models trained on code. *arXiv preprint arXiv:2107.03374*, 2021.
- Dasigi, P., Lo, K., Beltagy, I., Cohan, A., Smith, N. A., and Gardner, M. A dataset of information-seeking questions and answers anchored in research papers. In Toutanova, K., Rumshisky, A., Zettlemoyer, L., Hakkani-Tur, D., Beltagy, I., Bethard, S., Cotterell, R., Chakraborty, T., and Zhou, Y. (eds.), *Proceedings of the 2021 Conference of the North American Chapter of the Association for Computational Linguistics: Human Language Technologies*, pp. 4599–4610, Online, June 2021. Association for Computational Linguistics. doi: 10.18653/v1/2021.naacl-main.365. URL <https://aclanthology.org/2021.naacl-main.365/>.
- Devoto, A., Jeblick, M., and Jégou, S. Expected attention: Kv cache compression by estimating attention from future queries distribution, 2025. URL <https://arxiv.org/abs/2510.00636>.
- Dubey, A., Jauhri, A., Pandey, A., Kadian, A., Al-Dahle, A., Letman, A., Mathur, A., Schelten, A., Yang, A., Fan, A., et al. The llama 3 herd of models. *arXiv preprint arXiv:2407.21783*, 2024.
- Fabbri, A., Li, I., She, T., Li, S., and Radev, D. Multi-news: A large-scale multi-document summarization dataset and abstractive hierarchical model. In Korhonen, A., Traum, D., and Màrquez, L. (eds.), *Proceedings of the 57th Annual Meeting of the Association for Computational Linguistics*, pp. 1074–1084, Florence, Italy, July 2019. Association for Computational Linguistics. doi: 10.18653/v1/P19-1102. URL <https://aclanthology.org/P19-1102/>.
- Feng, Y., Lv, J., Cao, Y., Xie, X., and Zhou, S. K. Ada-kv: Optimizing KV cache eviction by adaptive budget allocation for efficient LLM inference. *CoRR*, abs/2407.11550, 2024. doi: 10.48550/ARXIV.2407.11550. URL <https://doi.org/10.48550/arXiv.2407.11550>.
- Feng, Y., Lv, J., Cao, Y., Xie, X., and Zhou, S. K. Identify critical KV cache in LLM inference from an output perturbation perspective. *CoRR*, abs/2502.03805, 2025. doi: 10.48550/ARXIV.2502.03805. URL <https://doi.org/10.48550/arXiv.2502.03805>.
- Fu, Y., Cai, Z., Asi, A., Xiong, W., Dong, Y., and Xiao, W. Not all heads matter: A head-level KV cache compression method with integrated retrieval and reasoning. In *The Thirteenth International Conference on Learning Representations, ICLR 2025, Singapore, April 24-28, 2025*. OpenReview.net, 2025. URL <https://openreview.net/forum?id=FJFVmeXusW>.
- Gliwa, B., Mochol, I., Biesek, M., and Wawer, A. SAM-Sum corpus: A human-annotated dialogue dataset for abstractive summarization. In Wang, L., Cheung, J. C. K., Carenini, G., and Liu, F. (eds.), *Proceedings of the 2nd Workshop on New Frontiers in Summarization*, pp. 70–79, Hong Kong, China, November 2019. Association for Computational Linguistics. doi: 10.18653/v1/D19-5409. URL <https://aclanthology.org/D19-5409/>.
- Ho, X., Duong Nguyen, A.-K., Sugawara, S., and Aizawa, A. Constructing a multi-hop QA dataset for comprehensive evaluation of reasoning steps. In Scott, D., Bel, N., and Zong, C. (eds.), *Proceedings of the 28th International Conference on Computational Linguistics*, pp. 6609–6625, Barcelona, Spain (Online), December 2020. International Committee on Computational Linguistics. doi: 10.18653/v1/2020.coling-main.580. URL <https://aclanthology.org/2020.coling-main.580/>.
- Hsieh, C.-P., Sun, S., Kriman, S., Acharya, S., Rekish, D., Jia, F., Zhang, Y., and Ginsburg, B. Ruler: What’s the real context size of your long-context language models? *arXiv preprint arXiv:2404.06654*, 2024.
- Huang, L., Cao, S., Parulian, N., Ji, H., and Wang, L. Efficient attentions for long document summarization. In Toutanova, K., Rumshisky, A., Zettlemoyer, L., Hakkani-Tur, D., Beltagy, I., Bethard, S., Cotterell, R., Chakraborty, T., and Zhou, Y. (eds.), *Proceedings of the 2021 Conference of the North American Chapter of the Association for Computational Linguistics: Human Language Technologies*, pp. 1419–1436, Online, June 2021. Association for Computational Linguistics. doi: 10.18653/v1/2021.naacl-main.112. URL <https://aclanthology.org/2021.naacl-main.112/>.
- Jiang, A. Q., Sablayrolles, A., Mensch, A., Bamford, C., Chaplot, D. S., Casas, D. d. l., Bressand, F., Lengyel, G., Lample, G., Saulnier, L., et al. Mistral 7b. *arXiv preprint arXiv:2310.06825*, 2023.

- Joshi, M., Choi, E., Weld, D., and Zettlemoyer, L. TriviaQA: A large scale distantly supervised challenge dataset for reading comprehension. In Barzilay, R. and Kan, M.-Y. (eds.), *Proceedings of the 55th Annual Meeting of the Association for Computational Linguistics (Volume 1: Long Papers)*, pp. 1601–1611, Vancouver, Canada, July 2017. Association for Computational Linguistics. doi: 10.18653/v1/P17-1147. URL <https://aclanthology.org/P17-1147/>.
- Kim, J., Kim, J., Kwon, S., Lee, J. W., Yun, S., and Song, H. O. Kvzip: Query-agnostic KV cache compression with context reconstruction. *CoRR*, abs/2505.23416, 2025. doi: 10.48550/ARXIV.2505.23416. URL <https://doi.org/10.48550/arXiv.2505.23416>.
- Kočiškỳ, T., Schwarz, J., Blunsom, P., Dyer, C., Hermann, K. M., Melis, G., and Grefenstette, E. The narrativeqa reading comprehension challenge. *Transactions of the Association for Computational Linguistics*, 6:317–328, 2018.
- Li, X. and Roth, D. Learning question classifiers. In *COLING 2002: The 19th International Conference on Computational Linguistics*, 2002. URL <https://aclanthology.org/C02-1150/>.
- Li, Y., Huang, Y., Yang, B., Venkitesh, B., Locatelli, A., Ye, H., Cai, T., Lewis, P., and Chen, D. Snapkv: LLM knows what you are looking for before generation. In Globersons, A., Mackey, L., Belgrave, D., Fan, A., Paquet, U., Tomczak, J. M., and Zhang, C. (eds.), *Advances in Neural Information Processing Systems 38: Annual Conference on Neural Information Processing Systems 2024, NeurIPS 2024, Vancouver, BC, Canada, December 10 - 15, 2024*, 2024. URL http://papers.nips.cc/paper_files/paper/2024/hash/28ab418242603e0f7323e54185d19bde-Abstract-Conference.html.
- Liu, T., Xu, C., and McAuley, J. Repobench: Benchmarking repository-level code auto-completion systems. *arXiv preprint arXiv:2306.03091*, 2023.
- NVIDIA. Kvpress, 2024. URL <https://github.com/NVIDIA/kvpress>.
- Park, J., Jones, D., Morse, M. J., Goel, R., Lee, M., and Lott, C. Keydiff: Key similarity-based KV cache eviction for long-context LLM inference in resource-constrained environments. *CoRR*, abs/2504.15364, 2025. doi: 10.48550/ARXIV.2504.15364. URL <https://doi.org/10.48550/arXiv.2504.15364>.
- Qin, Z., Cao, Y., Lin, M., Hu, W., Fan, S., Cheng, K., Lin, W., and Li, J. CAKE: cascading and adaptive KV cache eviction with layer preferences. In *The Thirteenth International Conference on Learning Representations, ICLR 2025, Singapore, April 24-28, 2025*. OpenReview.net, 2025. URL <https://openreview.net/forum?id=EQgEMAD4kv>.
- Rajpurkar, P., Jia, R., and Liang, P. Know what you don’t know: Unanswerable questions for SQuAD. In Gurevych, I. and Miyao, Y. (eds.), *Proceedings of the 56th Annual Meeting of the Association for Computational Linguistics (Volume 2: Short Papers)*, pp. 784–789, Melbourne, Australia, July 2018. Association for Computational Linguistics. doi: 10.18653/v1/P18-2124. URL <https://aclanthology.org/P18-2124/>.
- Team, Q. Qwen2.5: A party of foundation models, September 2024. URL <https://qwenlm.github.io/blog/qwen2.5/>.
- Trivedi, H., Balasubramanian, N., Khot, T., and Sabharwal, A. Musique: Multihop questions via single-hop question composition. *Transactions of the Association for Computational Linguistics*, 10:539–554, 2022.
- Xiao, G., Tian, Y., Chen, B., Han, S., and Lewis, M. Efficient streaming language models with attention sinks. In *The Twelfth International Conference on Learning Representations, ICLR 2024, Vienna, Austria, May 7-11, 2024*. OpenReview.net, 2024. URL <https://openreview.net/forum?id=NG7sS51zVF>.
- Yang, Z., Qi, P., Zhang, S., Bengio, Y., Cohen, W., Salakhutdinov, R., and Manning, C. D. HotpotQA: A dataset for diverse, explainable multi-hop question answering. In Riloff, E., Chiang, D., Hockenmaier, J., and Tsujii, J. (eds.), *Proceedings of the 2018 Conference on Empirical Methods in Natural Language Processing*, pp. 2369–2380, Brussels, Belgium, October–November 2018. Association for Computational Linguistics. doi: 10.18653/v1/D18-1259. URL <https://aclanthology.org/D18-1259/>.
- Zhang, Z., Sheng, Y., Zhou, T., Chen, T., Zheng, L., Cai, R., Song, Z., Tian, Y., Ré, C., Barrett, C. W., Wang, Z., and Chen, B. H2O: heavy-hitter oracle for efficient generative inference of large language models. In Oh, A., Naumann, T., Globerson, A., Saenko, K., Hardt, M., and Levine, S. (eds.), *Advances in Neural Information Processing Systems 36: Annual Conference on Neural Information Processing Systems 2023, NeurIPS 2023, New Orleans, LA, USA, December 10 - 16, 2023*, 2023. URL http://papers.nips.cc/paper_files/paper/2023/hash/6ceefa7b15572587b78ecfceb2827f8-Abstract-Conference.html.
- Zhong, M., Yin, D., Yu, T., Zaidi, A., Mutuma, M., Jha, R., Hassan, A., Celikyilmaz, A., Liu, Y., Qiu, X., et al. Qm-

sum: A new benchmark for query-based multi-domain meeting summarization. In *Proceedings of the 2021 Conference of the North American Chapter of the Association for Computational Linguistics: Human Language Technologies*, pp. 5905–5921, 2021.

A. Theoretical Proofs

A.1. Non-convexity of Eviction Loss in Eq. 8

Fix an attention head (ℓ, h) and consider the discrete loss sequence $\left\{ \mathcal{L}_{\ell, h} \left(\mathcal{M}_{\ell, h}^{\pi}(i) \right) \right\}_{i=0}^T$, where $\mathcal{M}_{\ell, h}^{\pi}(i)$ denotes the top- i positions selected by π in this head. Since $\mathcal{M}_{\ell, h}^{\pi}(i-1) \subset \mathcal{M}_{\ell, h}^{\pi}(i)$ and $\left| \mathcal{M}_{\ell, h}^{\pi}(i) \setminus \mathcal{M}_{\ell, h}^{\pi}(i-1) \right| = 1$ for all $i \geq 1$, by Eq. (6) we have

$$\begin{aligned} \mathcal{L}_{\ell, h} \left(\mathcal{M}_{\ell, h}^{\pi}(i) \right) &= \sum_{j \notin \mathcal{M}_{\ell, h}^{\pi}(i)} I_{\ell, h, j} \\ &= \sum_{j \notin \mathcal{M}_{\ell, h}^{\pi}(i-1)} I_{\ell, h, j} - \sum_{j \in \mathcal{M}_{\ell, h}^{\pi}(i) \setminus \mathcal{M}_{\ell, h}^{\pi}(i-1)} I_{\ell, h, j} \\ &= \mathcal{L}_{\ell, h} \left(\mathcal{M}_{\ell, h}^{\pi}(i-1) \right) - \sum_{j \in \mathcal{M}_{\ell, h}^{\pi}(i) \setminus \mathcal{M}_{\ell, h}^{\pi}(i-1)} I_{\ell, h, j}. \end{aligned} \quad (12)$$

Therefore, the discrete first difference is non-positive:

$$\mathcal{L}_{\ell, h} \left(\mathcal{M}_{\ell, h}^{\pi}(i) \right) - \mathcal{L}_{\ell, h} \left(\mathcal{M}_{\ell, h}^{\pi}(i-1) \right) = - \sum_{j \in \mathcal{M}_{\ell, h}^{\pi}(i) \setminus \mathcal{M}_{\ell, h}^{\pi}(i-1)} I_{\ell, h, j} \leq 0. \quad (13)$$

The discrete second difference satisfies

$$\begin{aligned} &\mathcal{L}_{\ell, h} \left(\mathcal{M}_{\ell, h}^{\pi}(i+1) \right) - 2\mathcal{L}_{\ell, h} \left(\mathcal{M}_{\ell, h}^{\pi}(i) \right) + \mathcal{L}_{\ell, h} \left(\mathcal{M}_{\ell, h}^{\pi}(i-1) \right) \\ &= \left(\mathcal{L}_{\ell, h} \left(\mathcal{M}_{\ell, h}^{\pi}(i+1) \right) - \mathcal{L}_{\ell, h} \left(\mathcal{M}_{\ell, h}^{\pi}(i) \right) \right) - \left(\mathcal{L}_{\ell, h} \left(\mathcal{M}_{\ell, h}^{\pi}(i) \right) - \mathcal{L}_{\ell, h} \left(\mathcal{M}_{\ell, h}^{\pi}(i-1) \right) \right) \\ &= \sum_{j \in \mathcal{M}_{\ell, h}^{\pi}(i) \setminus \mathcal{M}_{\ell, h}^{\pi}(i-1)} I_{\ell, h, j} - \sum_{j \in \mathcal{M}_{\ell, h}^{\pi}(i+1) \setminus \mathcal{M}_{\ell, h}^{\pi}(i)} I_{\ell, h, j}. \end{aligned} \quad (14)$$

Hence, $\mathcal{L}_{\ell, h} \left(\mathcal{M}_{\ell, h}^{\pi}(i) \right)$ is (discretely) convex in i if and only if the increment added at step i has no smaller oracle importance than the increment added at step $i+1$, i.e., the oracle importances are non-increasing along the ordering induced by π . For a heuristic metric π , this monotonicity generally fails (there exist inversions w.r.t. $I_{\ell, h, \cdot}$), which implies that there exists some i such that the right-hand side of Eq. (14) is negative. Consequently, $\mathcal{L}_{\ell, h} \left(\mathcal{M}_{\ell, h}^{\pi}(b_{\ell, h}) \right)$ is non-convex as a function of $b_{\ell, h}$ in general, and Eq. (8) is a non-convex combinatorial optimization problem.

A.2. Convex Relaxation Optimization of Equation 8

Eq. (8) is a discrete multi-head budget allocation problem. As shown in Appendix A.1, for a heuristic metric π , $\mathcal{L}_{\ell, h} \left(\mathcal{M}_{\ell, h}^{\pi}(b_{\ell, h}) \right)$ is generally non-convex in $b_{\ell, h}$. We adopt the convex-hull relaxation described in Section 4.2 to obtain a tractable surrogate objective.

Convex surrogate loss by PAVA. For each head (ℓ, h) , consider the raw discrete loss sequence $\left\{ \mathcal{L}_{\ell, h} \left(\mathcal{M}_{\ell, h}^{\pi}(i) \right) \right\}_{i=0}^T$. Applying isotonic regression via PAVA yields a convex, non-increasing surrogate sequence $\left\{ \check{\mathcal{L}}_{\ell, h} \left(\mathcal{M}_{\ell, h}^{\pi}(i) \right) \right\}_{i=0}^T$, as defined in Section 4.2. We further define the effective marginal gain (Eq. (9)) as

$$g_{\ell, h}^{\pi}(i) = \check{\mathcal{L}}_{\ell, h} \left(\mathcal{M}_{\ell, h}^{\pi}(i-1) \right) - \check{\mathcal{L}}_{\ell, h} \left(\mathcal{M}_{\ell, h}^{\pi}(i) \right) \geq 0, \quad (15)$$

which is monotonically non-increasing in i .

Equivalent maximization form. By telescoping Eq. (15), for any integer budget $b_{\ell, h} \in \{0, 1, \dots, T\}$ we have

$$\check{\mathcal{L}}_{\ell, h} \left(\mathcal{M}_{\ell, h}^{\pi}(b_{\ell, h}) \right) = \check{\mathcal{L}}_{\ell, h} \left(\mathcal{M}_{\ell, h}^{\pi}(0) \right) - \sum_{i=1}^{b_{\ell, h}} g_{\ell, h}^{\pi}(i). \quad (16)$$

Substituting Eq. (16) into Eq. (10), the relaxed minimization is equivalent to the following maximization:

$$\max_{\{b_{\ell,h}\}} \sum_{\ell=1}^L \sum_{h=1}^H \sum_{i=1}^{b_{\ell,h}} g_{\ell,h}^{\pi}(i) \quad \text{s.t.} \quad \sum_{\ell=1}^L \sum_{h=1}^H b_{\ell,h} = B_{\text{total}}. \quad (17)$$

Optimality of greedy allocation. Since $g_{\ell,h}^{\pi}(i)$ is non-increasing in i for every head, Eq. (17) is a separable diminishing-returns allocation problem. An optimal solution is obtained by iteratively allocating one unit of budget to the head (ℓ, h) that maximizes the next available gain $g_{\ell,h}^{\pi}(b_{\ell,h} + 1)$, until the budget constraint is met. Equivalently, the greedy procedure selects the B_{total} largest feasible marginal gains across all heads under the prefix constraint induced by $\{g_{\ell,h}^{\pi}(i)\}_i$, which yields the global optimum of Eq. (10).

B. Additional Experimental Results

B.1. Visualizing the Eviction Loss across Different Metrics

To evaluate the universality of the *optimality gap*, we visualize the eviction loss for the **Mistral-7B-v0.3** model on the **HotpotQA** task (**LongBench**) under an 80% global compression ratio. Figure 6 illustrates the results across three heuristic metrics: **SnapKV**, **KeyDiff**, and **EA**.

B.2. Comprehensive Head-wise Optimal Allocation Profiles

In this section, we provide the full visualization of the **optimal budget allocation profiles** for the *Mistral-7B-v0.3* model using the **KeyDiff** metric. These figures display the mapping from the target global compression ratio to the allocated local compression ratio for each of the 32 layers and 8 heads.

The elements in the visualizations are defined as follows:

- The **horizontal axis** (*x-axis*) represents the **Global Compression Ratio** ($\sigma \in [0, 1]$).
- The **vertical axis** (*y-axis*) represents the **Optimal Local Compression Ratio** ($r_{\ell,h}$) for the specific head.
- The **black solid line** (labeled as ‘mytest convex’) indicates the allocation curve derived from our proposed **convex-hull optimization** algorithm, calculated using our synthetic calibration data.
- The **orange dashed line** (labeled as ‘mytest mckp’) represents the theoretical optimal solution computed via the **Multi-Choice Knapsack Problem (MCKP)** dynamic programming algorithm on the synthetic calibration data.
- The **background colored lines** represent the corresponding utility profiles for various downstream datasets in the benchmark.

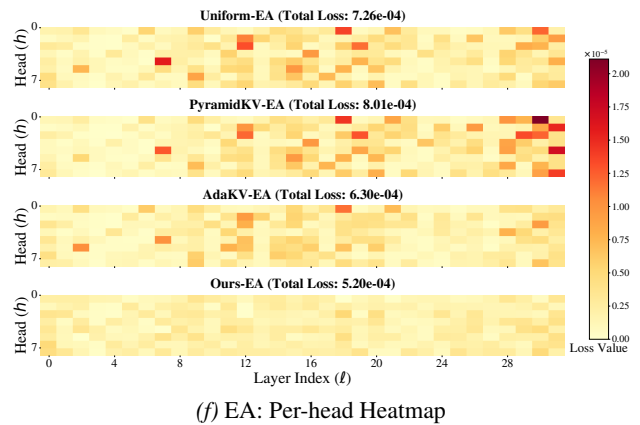
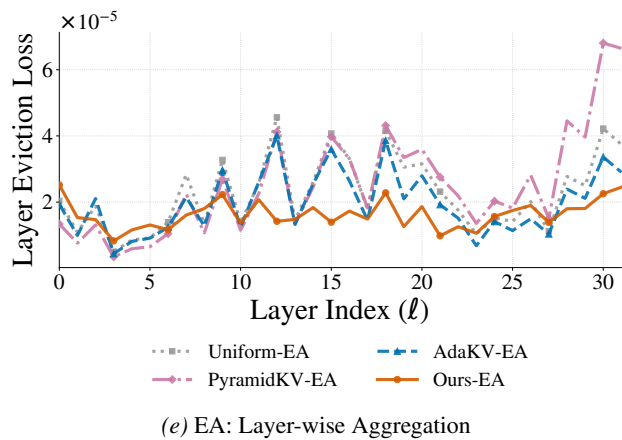
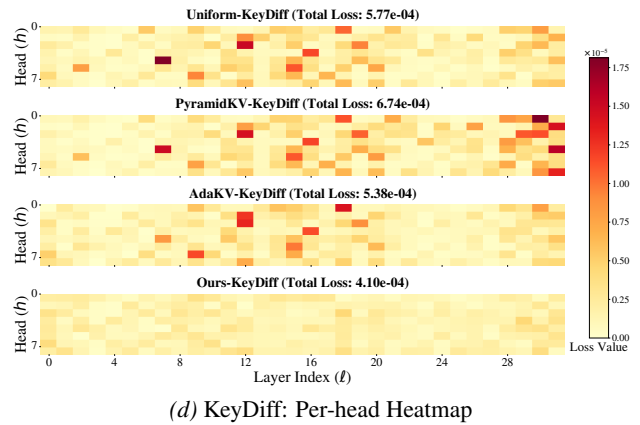
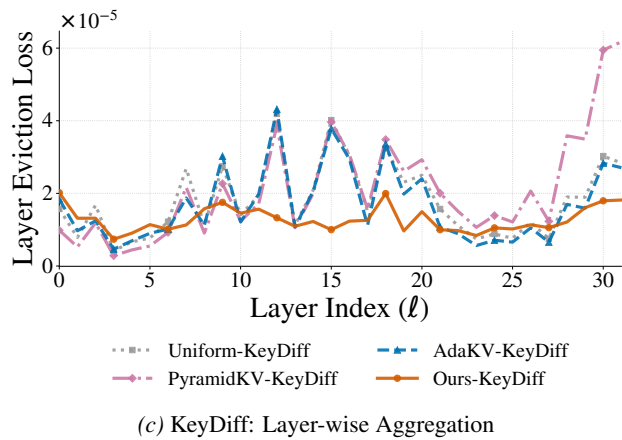
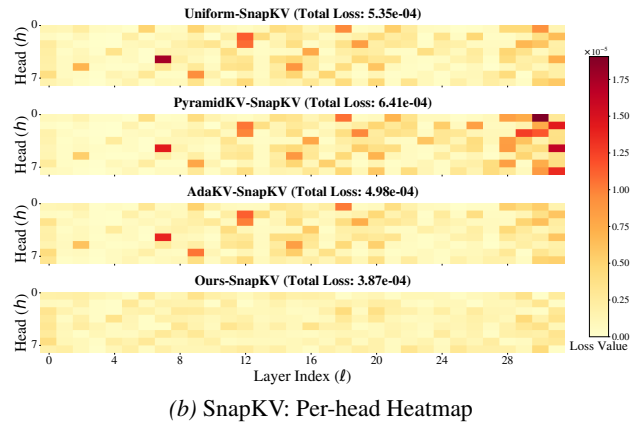
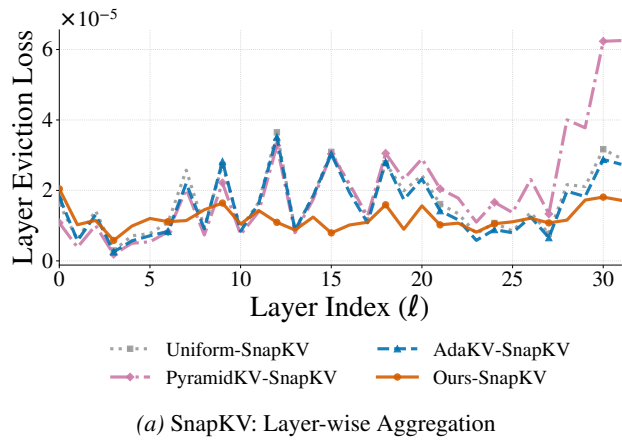


Figure 6. Performance of Mistral-7B-v0.3 on HotpotQA (LongBench) across different metrics. The figure compares the aggregated layer-wise eviction loss (left column) and per-head loss distribution heatmaps (right column) for SnapKV (top row), KeyDiff (middle row), and EA (bottom row) at an 80% global compression ratio.

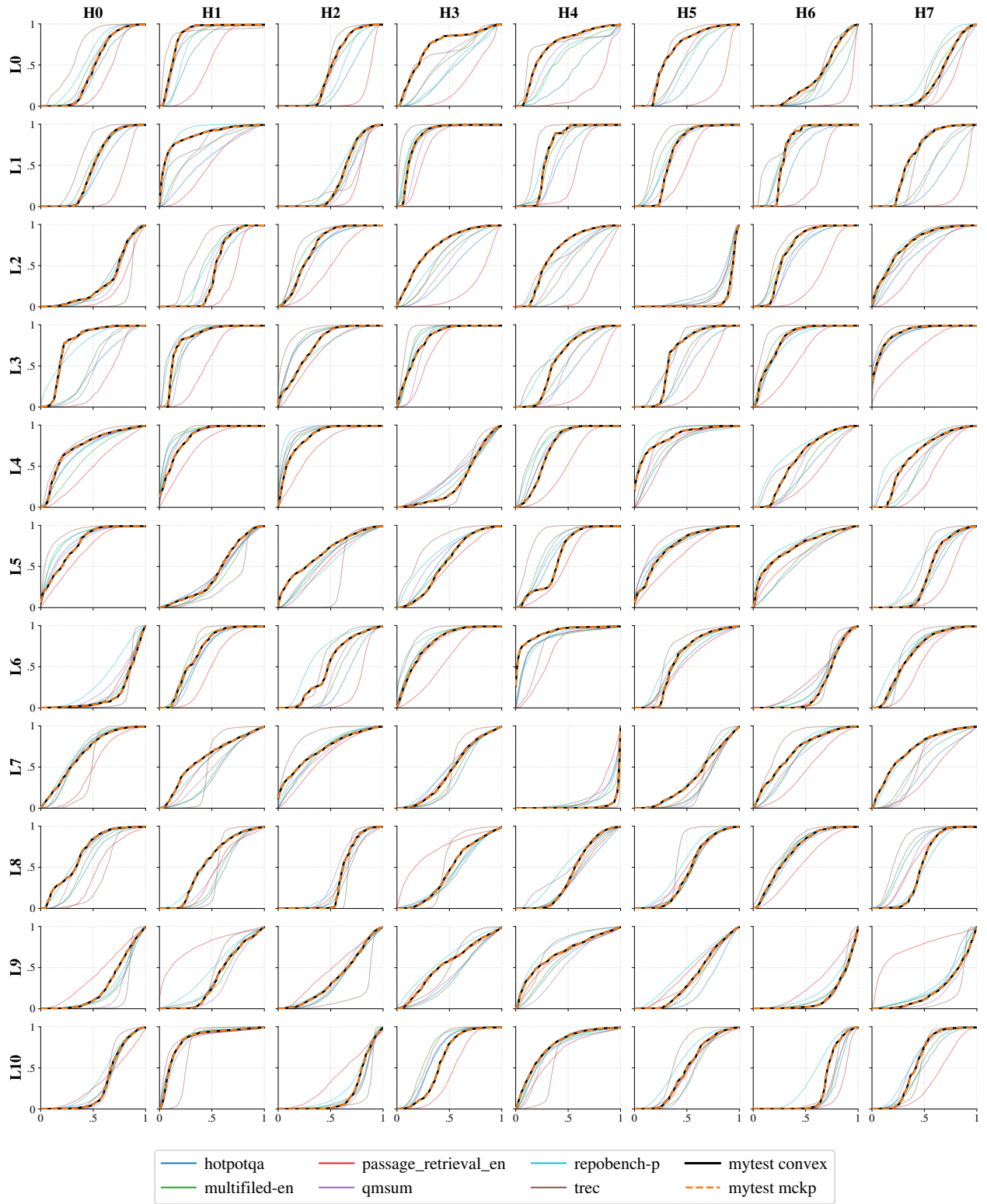


Figure 7. **Head-wise Optimal Allocation Profiles (Part I: Layers 0 to 10).** Visualization of the optimal local budget distribution for the **Mistral-7B-v0.3** model on the different tasks (LongBench) using the **KeyDiff** metric.

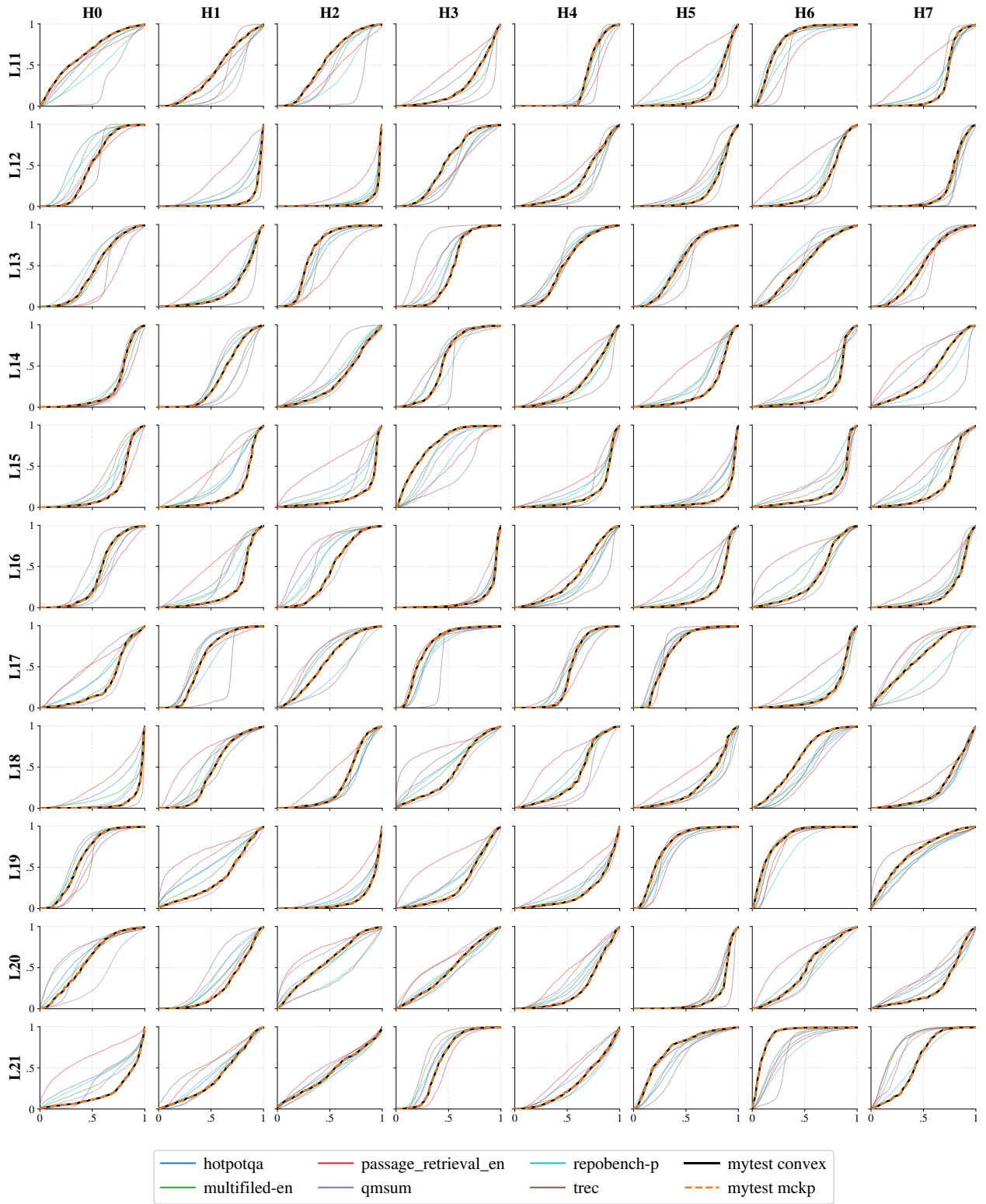


Figure 8. Head-wise Optimal Allocation Profiles (Part II: Layers 11 to 21). Visualization of the optimal local budget distribution for the **Mistral-7B-v0.3** model on the different tasks (LongBench) using the **KeyDiff** metric.

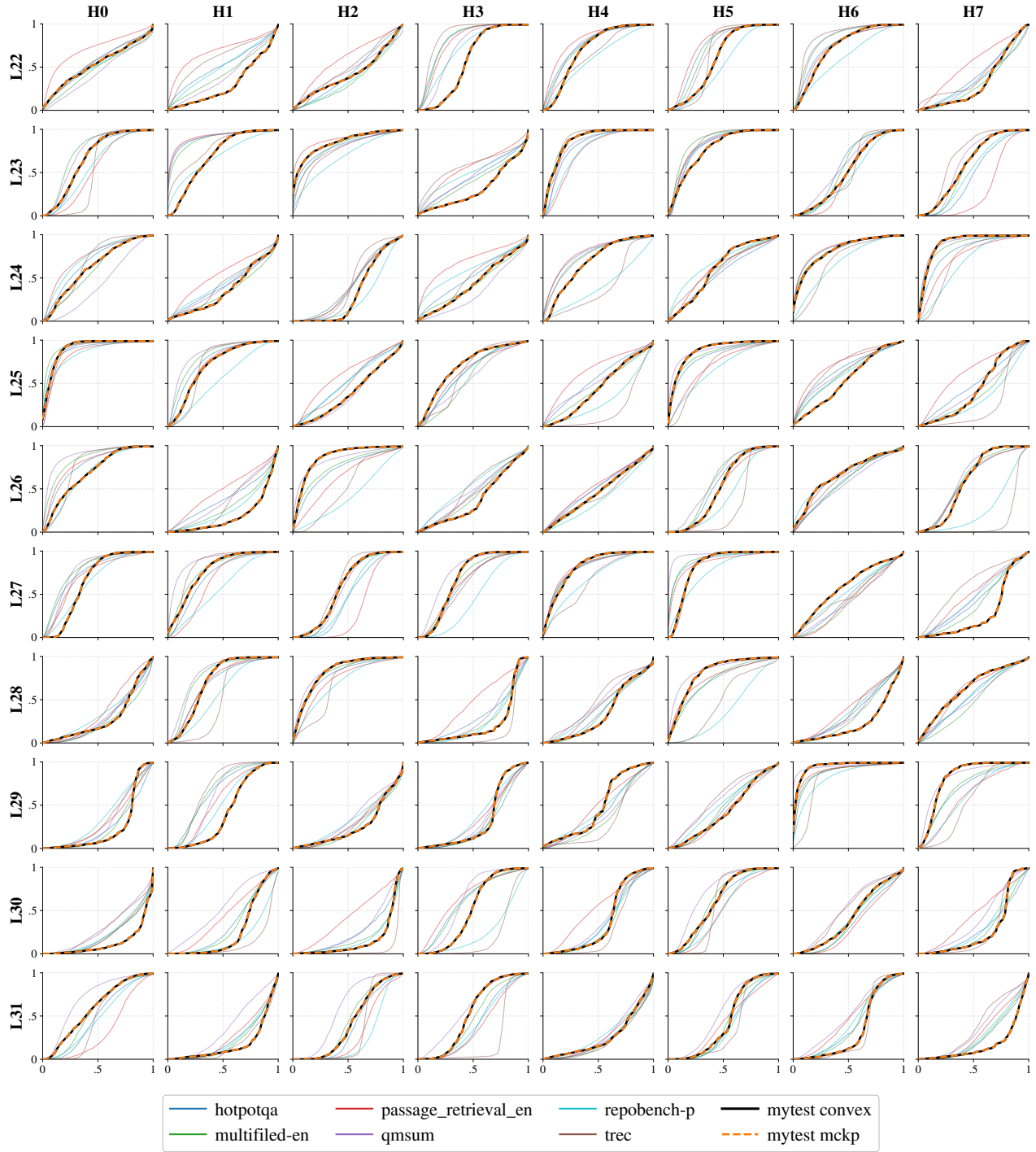


Figure 9. Head-wise Optimal Allocation Profiles (Part III: Layers 22 to 31). Visualization of the optimal local budget distribution for the Mistral-7B-v0.3 model on the different tasks (LongBench) using the KeyDiff metric.

Predicting Future Utility: Global Combinatorial Optimization for Task-Agnostic KV Cache Eviction

Table 4. Detailed scores of 16 datasets on LongBench at an 50% compression ratio.

Model	Method	Single-Doc QA			Multi-Doc QA			Summarization			Few-shot			Synthetic		Code		Avg
		NrvQA	Qasper	ME-en	Hoplot	2WikiQA	Mustique	GovRep	QMSum	MultiNews	TREC	TriviaQA	SAMSum	PCount	PR-en	Lcc	RB-P	
Mistral-7B-v0.3	Full-KV	27.04	38.30	49.75	49.11	36.68	27.69	34.64	25.55	26.40	76.50	88.96	47.11	5.50	97.00	65.60	60.92	47.30
	<i>Metric SnapKV</i> (π_1)																	
	Uniform- π_1	24.51	32.14	42.98	48.71	34.72	24.64	32.07	23.68	25.10	68.50	88.91	47.18	5.50	96.50	65.36	60.51	45.06
	Pyramid- π_1	24.40	30.30	44.34	48.54	34.10	24.18	31.74	24.06	24.43	67.50	89.21	46.83	3.50	97.50	65.63	60.34	44.79
	Ada- π_1	24.47	31.50	43.61	50.00	35.93	25.43	31.51	24.27	25.11	72.00	88.94	47.29	6.50	96.50	65.35	60.87	45.58
	LU-KV-π_1 (Ours)	25.81	38.93	50.53	49.20	36.82	27.05	34.96	25.64	26.42	76.00	89.45	47.33	5.54	98.00	66.14	61.62	47.46
	<i>Metric KeyDiff</i> (π_2)																	
	Uniform- π_2	24.03	35.36	49.01	47.61	36.29	25.34	31.97	24.38	25.46	56.00	88.56	46.57	4.20	95.00	56.82	60.52	44.20
	Pyramid- π_2	27.26	34.78	46.46	45.38	35.94	25.21	31.73	24.84	25.35	68.00	89.21	47.31	6.50	96.00	47.92	60.37	44.52
	Ada- π_2	26.05	37.68	51.31	47.04	37.79	26.43	33.02	25.05	25.80	63.00	88.39	46.82	2.87	95.25	65.27	60.39	45.76
	LU-KV-π_2 (Ours)	27.66	38.91	50.92	51.30	39.67	24.42	34.57	25.48	26.60	75.00	89.46	47.61	3.05	95.75	63.24	61.14	47.17
Llama-3.1-8B	Full-KV	29.39	45.17	55.74	58.31	48.12	32.57	34.53	25.30	26.91	72.50	91.78	44.32	8.47	99.50	63.43	52.59	49.29
	<i>Metric SnapKV</i> (π_1)																	
	Uniform- π_1	26.46	39.37	48.32	56.53	44.99	30.41	31.75	23.65	25.30	62.50	92.31	44.01	7.00	99.50	66.01	53.89	47.00
	Pyramid- π_1	28.13	33.86	48.94	55.26	46.16	31.36	30.80	24.58	24.23	60.00	92.53	44.03	6.59	99.50	65.98	54.44	46.65
	Ada- π_1	29.32	40.23	51.32	56.01	44.67	32.38	31.82	24.23	25.40	68.50	91.90	44.19	7.89	99.50	64.92	54.31	47.91
	LU-KV-π_1 (Ours)	30.57	44.45	55.59	56.91	47.32	32.33	34.64	25.40	26.64	71.50	91.65	44.14	7.95	100.00	65.25	55.77	49.38
	<i>Metric KeyDiff</i> (π_2)																	
	Uniform- π_2	30.58	41.13	52.39	55.78	43.72	29.92	32.73	24.68	25.07	65.00	92.03	45.07	7.83	99.50	55.89	54.58	47.24
	Pyramid- π_2	30.66	41.15	52.06	56.13	44.73	30.01	31.85	25.11	24.98	59.00	91.78	45.18	6.08	99.50	37.66	55.42	45.71
	Ada- π_2	31.24	43.64	51.53	52.68	48.46	31.66	34.06	24.38	26.06	70.00	91.11	44.80	7.08	99.50	63.68	56.85	48.55
	LU-KV-π_2 (Ours)	29.78	44.14	54.23	54.67	44.59	27.43	34.71	25.35	26.63	74.00	91.89	44.52	5.79	99.50	63.75	54.52	48.47
Qwen2.5-32B	Full-KV	30.68	45.93	52.13	63.00	60.75	38.71	32.43	24.51	25.06	72.00	88.71	46.01	11.50	100.00	50.72	33.98	48.51
	<i>Metric SnapKV</i> (π_1)																	
	Uniform- π_1	28.40	36.02	44.58	62.89	57.71	37.40	30.95	22.17	23.92	67.50	89.02	45.16	13.00	99.50	55.52	34.83	46.79
	Pyramid- π_1	25.81	22.00	36.10	57.36	49.10	33.74	28.95	21.71	21.41	58.00	89.03	45.55	10.00	100.00	60.03	35.60	43.40
	Ada- π_1	27.16	34.67	43.39	63.10	57.34	36.58	30.84	22.02	23.95	70.50	88.82	45.67	11.50	99.75	54.38	33.63	46.46
	LU-KV-π_1 (Ours)	30.73	44.26	51.59	63.21	60.75	39.74	31.96	24.02	24.72	71.50	88.38	45.40	12.00	100.00	59.30	37.70	49.08
	<i>Metric KeyDiff</i> (π_2)																	
	Uniform- π_2	28.66	37.44	47.88	62.21	58.97	39.09	30.86	23.53	23.37	75.00	85.93	46.15	13.25	98.00	41.03	34.73	46.63
	Pyramid- π_2	27.84	30.57	40.25	55.92	50.81	32.99	28.69	22.47	21.50	65.50	86.66	45.14	9.67	75.08	25.86	35.40	40.90
	Ada- π_2	29.90	42.44	51.13	60.14	59.78	39.67	31.90	23.21	23.96	72.00	87.23	44.84	13.50	100.00	43.33	33.71	47.30
	LU-KV-π_2 (Ours)	31.63	45.78	51.38	63.37	63.00	43.18	32.46	24.69	25.04	74.00	89.26	44.47	10.50	100.00	53.40	34.51	49.17

B.3. Detailed Scores Of LongBench

In this section, we provide a comprehensive breakdown of performance across all 16 datasets in *LongBench*. Table 4 presents the results under a 50% global compression ratio for **SnapKV** (π_1) and **KeyDiff** (π_2) metrics. To further verify the universality of our approach under more aggressive compression, we also evaluate the performance at an 80% global compression ratio in Table 5, extending our analysis to include the **EA** (π_3) metric. Across these diverse settings, different importance metrics, and various model scales, the results consistently demonstrate that our proposed method remains effective.

B.4. Detailed Scores Of RULER

In this section, we provide a detailed performance breakdown on the **RULER** benchmark, evaluating the model across both RULER-16K (Table 6) and RULER-4K (Table 7). These evaluations are conducted at a strict 80% global compression ratio and include the **EA** (π_3) metric to test the robustness of our method in extreme retrieval scenarios.

The results show that traditional baselines, such as *Uniform* and *PyramidKV*, experience significant performance degradation in complex tasks like *multikey* and *variable-tracking* (vt). While *AdaKV* provides some improvement in specific configurations, it remains sensitive to the underlying heuristic metric. This is particularly evident with the **EA** metric; for example, on *Mistral-7B-v0.3* (RULER-16K), *AdaKV* achieves only 26.28% average accuracy.

In contrast, our proposed method (**LU-KV**) consistently achieves superior results across all tasks and metrics. By effectively optimizing the budget allocation, our method significantly boosts retrieval accuracy. Notably, in the aforementioned *Mistral-EA* setting, our method improves the average accuracy to **68.60%**. Similar performance gains are observed for *Llama-3.1-8B* and *Qwen2.5-32B*, confirming the effectiveness of our approach across different model scales and importance metrics.

C. Details about Benchmarks

To evaluate the long-context capabilities of the models comprehensively, we employ two distinct benchmarks: RULER and LongBench. These benchmarks provide complementary insights, with RULER offering controllable synthetic stress tests and LongBench providing realistic multi-task evaluations.

C.1. RULER

RULER (Hsieh et al., 2024) is a synthetic benchmark designed to evaluate long-context language models beyond the standard retrieval-based “needle-in-a-haystack” (NIAH) tests. Unlike simple retrieval tasks, RULER introduces flexible configurations to customize sequence length and task complexity. It categorizes tasks into four distinct domains to test behaviors beyond searching from context:

- **Retrieval:** Extending the vanilla NIAH, this category includes Single NIAH (S-NIAH), Multi-keys NIAH (MK-NIAH), Multi-values NIAH (MV-NIAH), and Multi-queries NIAH (MQ-NIAH). These tasks test the model’s robustness against distractors and its ability to retrieve diverse types and quantities of needles.
- **Multi-hop Tracing:** To evaluate coreference chain resolution, RULER utilizes a Variable Tracking (VT) task, requiring the model to trace variable assignment chains across the long context.
- **Aggregation:** This category tests the ability to aggregate relevant information spanning long-range context. Tasks include Common Words Extraction (CWE) and Frequent Words Extraction (FWE), where the model identifies words based on their frequency distribution.
- **Question Answering (QA):** This domain uses augmented versions of SQuAD (Rajpurkar et al., 2018) and HotpotQA (Yang et al., 2018) with inserted distractors to simulate long-context question answering scenarios.

C.2. LongBench

Complementing the synthetic nature of RULER, we utilize LongBench (Bai et al., 2024), a multi-task benchmark designed to assess long-context understanding in realistic scenarios. In this work, we focus specifically on the **16 English datasets** from LongBench, which cover six major task categories. The English subset comprises:

- **Single-Document QA:** Evaluated using NarrativeQA (Kočiskỳ et al., 2018), Qasper (Dasigi et al., 2021), and MultiFieldQA-en, requiring models to comprehend long individual documents.
- **Multi-Document QA:** Involves complex reasoning across multiple documents, utilizing HotpotQA (Yang et al., 2018), 2WikiMultihopQA (Ho et al., 2020), and MuSiQue (Trivedi et al., 2022).
- **Summarization:** Tests the ability to synthesize long inputs using GovReport (Huang et al., 2021), QMSum (Zhong et al., 2021), and MultiNews (Fabbri et al., 2019).
- **Few-Shot Learning:** Assesses in-context learning abilities with long-context examples from TREC (Li & Roth, 2002), TriviaQA (Joshi et al., 2017), and SAMSum (Gliwa et al., 2019).
- **Synthetic Tasks:** Includes PassageCount and PassageRetrieval-en to isolate specific long-range dependency capabilities.
- **Code Completion:** Evaluates programming context understanding using LCC (Chen, 2021) and RepoBench-P (Liu et al., 2023).

D. Details about Baselines

We adopted the original hyperparameters for the baseline methods as reported in their respective papers, details in Table 8.

Table 8. Hyperparameter configurations for baseline methods, following their original reports.

Method	Hyperparameters
SnapKV (Li et al., 2024)	Kernel size = 7, Window size = 32
AdaKV (Feng et al., 2024)	$\alpha_{\text{safeguard}} = 0.20$, Window size = 32
PyramidKV (Cai et al., 2024)	$\beta = 20$, Window size = 8
Expected Attention (Devoto et al., 2025)	$n_{\text{future.positions}} = 512$, $n_{\text{sink}} = 4$, $\epsilon = 0.02$

E. LU-KV Implementation Details

For offline calibration, we employed an AI-generated novel ($\approx 4,000$ words) paired with 30 generated questions. We utilized the L_2 -norm of the projected Value vectors ($|vW_O|_2$) for scoring, applying intra-layer normalization to the results. We configured the attention sink size to 4. The recent token window was set to 1 for KeyDiff and maintained at 32 for SnapKV. Additionally, we imposed a maximum compression threshold of 99% for any attention head, ensuring a minimum retention rate of 1%.